

Anomalous Flux Flow Resistivity in Two Gap Superconductor MgB₂

A. Shibata, M. Matsumoto, K. Izawa, and Y. Matsuda

*Institute for Solid State Physics, University of Tokyo,
Kashiwanoha 5-1-5, Kashiwa, Chiba 277-8581, Japan*

S. Lee, and S. Tajima

Superconductivity Research Laboratory, ISTEC, 1-10-13 Shinonome, Koto-ku, Tokyo 135-0062, Japan

(Dated: March 22, 2022)

The flux flow resistivity ρ_f associated with purely viscous motion of vortices in high-quality MgB₂ was measured by microwave surface impedance. Flux flow resistivity exhibits unusual field dependence with strong enhancement at low field, which is markedly different to conventional s -wave superconductors. A crossover field which separates two distinct flux flow regimes having different ρ_f slopes was clearly observed in $\mathbf{H} \parallel ab$ -plane. The unusual H -dependence indicates that two very differently sized superconducting gaps in MgB₂ manifest in the vortex dynamics and almost equally contribute to energy dissipation. The carrier scattering rate in two different bands is also discussed with the present results, compared to heat capacity and thermal conductivity results.

PACS numbers: 74.25.Fy, 74.25.Nf, 74.70.Ad

Since the recent discovery of high temperature superconductivity in MgB₂, great attention has been directed towards understanding the detailed nature of superconductivity [1, 2]. MgB₂ consists of two bands having roughly equal density of states (DOS), strongly two dimensional σ -band (sp_xp_y) and three dimensional π -band (p_z) bands. Associated with these two bands, two very differently sized superconducting gaps are quite distinct and manifest themselves clearly in many physical properties, which have become one of the central topic of the physical properties of MgB₂. In fact, apart from the much debated pairing mechanism of high transition temperature superconductivity, physical properties in the superconducting state *i.e.*, the distinguishing characteristics of a superconductor with two gaps, are still largely unexplored. Recent scanning tunneling microscope (STM) [3], heat capacity [4], and thermal conductivity [5] measurements have revealed that the physical properties in the vortex state of MgB₂ are dramatically different from those expected in conventional s -wave superconductors. Despite these extensive studies, however, the dynamical properties of the vortices, such as the energy dissipation associated with the vortex motion which is intimately related to the electronic structure [6, 7, 8, 9], are still far from being completely understood.

When a vortex line in a type-II superconductor responds to a driving current, frictional force is given by the damping viscosity, which in turn depends on the energy dissipation process of quasiparticles in and around the vortex cores. To gain an understanding of this energy dissipation, experimental determination of the free flux flow (FFF) resistivity is particularly important. FFF refers to a purely viscous vortex motion of vortices, which is realized when the vortices move in pinned free states. The FFF state in conventional s -wave superconductors has been extensively studied and a rather good understanding has been developed. In s -wave superconductors, quasiparticles trapped within the vortex core that form

Caroli-de Gennes-Matricon bound states play a key role in the dissipation process [6, 7]. The FFF resistivity ρ_f is essentially proportional to normal state resistivity ρ_n and applied field,

$$\rho_f = \frac{H}{H_{c2}} \rho_n. \quad (1)$$

This Bardeen-Stephen relationship has been confirmed in most dirty and clean s -wave systems throughout almost the whole Abrikosov phase. Recently, striking deviation of FFF resistivity from Eq.(1) has been reported in unconventional superconductors with gap nodes [8, 9, 10, 11, 12, 13]. For instance, in d -wave Bi₂Sr₂CuO_{6+ δ} , ρ_f exhibits a H -linear dependence at low fields, followed by a non-linear H -dependence described well by,

$$\rho_f \propto \sqrt{\frac{H}{H_{c2}}} \rho_n, \quad (2)$$

at higher fields [9]. This demonstrates that the energy dissipation is strongly influenced by the superconducting gap structure. However, despite these extensive studies of the FFF state, the detailed microscopic mechanism of energy dissipation is not well understood, exposing our incomplete knowledge of vortex dynamics. This situation thus calls for a new textbook example of FFF resistivity in a superconductor with a distinctive gap structure. The FFF resistivity of MgB₂ with two distinct superconducting gaps may provide an unique opportunity for studying how the energy dissipation occurs when vortices move in the superfluid.

In this paper, FFF resistivities of MgB₂ are examined by measuring microwave surface impedance. FFF resistivity exhibits unusual field dependence, which is markedly different from conventional s -wave superconductors. These results are discussed in terms of energy dissipation in the superconductors with two distinct gaps.

High quality single crystals of MgB₂ ($T_c=38.6$ K) were grown using a high pressure method [14]. Typical size

was $0.3 \times 0.3 \times 0.1 \text{ mm}^3$. Microwave surface impedance $Z_s = R_s + iX_s$, where R_s and X_s are the surface resistance and surface reactance, respectively, was measured by the standard cavity perturbation technique [15]. Cylindrical cavity resonators made of Cu ($Q \simeq 44000$) and superconducting Pb ($Q \simeq 1.0 \times 10^6$) operated at 28.5 GHz were used in TE₀₁₁ mode. Sample was placed in an antinode of the oscillatory magnetic field \mathbf{H}_ω . Z_s was measured in two different configurations, $\mathbf{H}_\omega \parallel \mathbf{H} \parallel c$ -axis ($Z_s^{H_\omega \parallel c}$) and $\mathbf{H}_\omega \parallel \mathbf{H} \parallel ab$ -plane ($Z_s^{H_\omega \parallel ab}$).

Figures 1 (a) and (b) show the T -dependence of in-plane and out-of-plane surface impedance, $Z_s^{ab} = R_s^{ab} + iX_s^{ab}$ and $Z_s^c = R_s^c + iX_s^c$, respectively, measured by Pb-resonator in the Meissner phase. Both sets of data were obtained by the measurements of $Z_s^{H_\omega \parallel c}$ and $Z_s^{H_\omega \parallel ab}$ (see the insets of Fig. 1). In the configuration $\mathbf{H}_\omega \parallel c$, $Z_s^{ab} = Z_s^{H_\omega \parallel c}$ because the oscillatory currents flow within the ab -plane. For $\mathbf{H}_\omega \parallel ab$, $Z_s^{H_\omega \parallel ab}$ is determined by the geometrical mean value of Z_s^{ab} and Z_s^c as $Z_s^{H_\omega \parallel ab} = \frac{S^{ab}Z_s^{ab} + S^cZ_s^c}{S^{ab} + S^c}$. Here S^{ab} and S^c are the areas of the faces where the screening currents flow in the ab -plane and along the c direction, respectively [16]. Since $S^{ab} \sim 3S^c$, and $Z_s^c \sim 1.7Z_s^{ab}$ from the anisotropy of normal state resistivities ($\rho_n^c/\rho_n^{ab} \sim 3$ [17]), Z_s^c and Z_s^{ab} make contribution in the same order to $Z_s^{H_\omega \parallel ab}$. In both configurations, both R_s and X_s decrease rapidly with decreasing T below T_c . In the Meissner phase, microwave response is purely reactive and $R_s \simeq 0$ and $X_s = \mu_0\omega\lambda$, where μ_0 is the permeability of free space, $\omega/2\pi$ is the microwave frequency, and λ is the London penetration length. On the other hand, response is dissipative in the normal state and $R_s = X_s = \mu_0\omega\delta_n/2$, where $\delta_n = \sqrt{2\rho_n/\mu_0\omega}$ is the

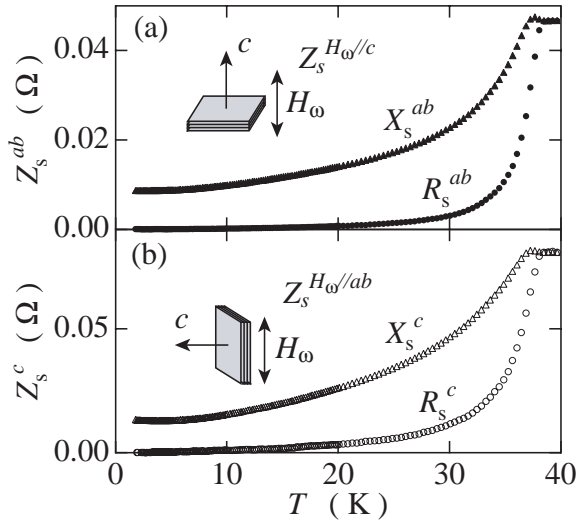


FIG. 1: (a) Temperature dependence of in-plane surface impedance, $Z_s^{ab} = R_s^{ab} + iX_s^{ab}$, in MgB₂ single crystal. (b) The same data for out-of-plane surface impedance, $Z_s^c = R_s^c + iX_s^c$. $\rho_n^{ab} = 2\mu\Omega \text{ cm}$, $\rho_n^c/\rho_n^{ab} = 3$ and $S^{ab} = 3S^c$ were used.

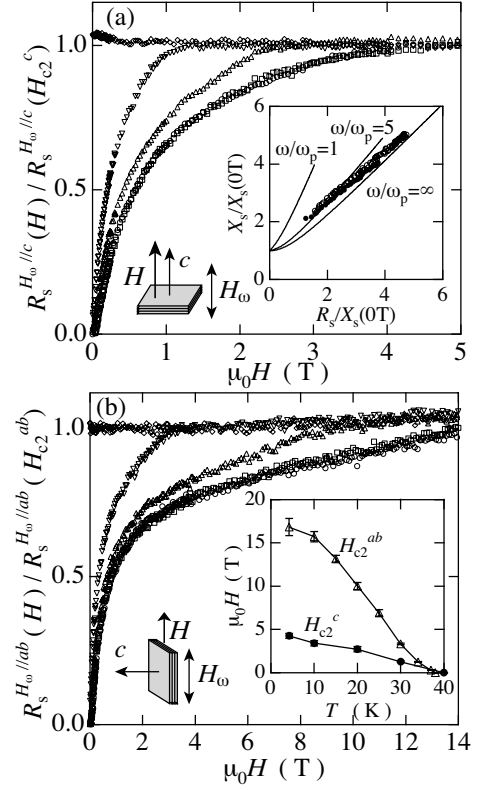


FIG. 2: (a) H -dependence of surface resistance $R_s^{H_\omega \parallel c}$ normalized by the normal state values measured in $\mathbf{H} \parallel \mathbf{H}_\omega \parallel c$ at 40 K (diamonds), 30 K (inverted triangles), 20 K (triangles), 10 K (squares), and 2.3 K (circles). Inset: A plot of impedance $R_s/X_s(0T)$ vs $X_s/X_s(0T)$ for $\mathbf{H} \parallel \mathbf{H}_\omega \parallel c$ (filled circles) and for $\mathbf{H} \parallel \mathbf{H}_\omega \parallel ab$ (open circles). The solid lines are the results calculated from Eq. (3) at different pinning frequencies. (b) The same plot for $R_s^{H_\omega \parallel ab}$ measured in $\mathbf{H} \parallel \mathbf{H}_\omega \parallel ab$. Inset: T -dependence of H_{c2}^{ab} and H_{c2}^c , as determined by the field at which R_s is the normal state value.

skin depth and ρ_n is the normal state resistivity. The absolute value of R_s^i and X_s^i ($i = ab$ and c) were determined by comparison with dc resistivity ρ_n^i assuming that $R_s^i = X_s^i = \sqrt{\mu_0\omega\rho_n^i}/2$ in the normal state. Using $\rho_n^{ab} \sim 2\mu\Omega \text{ cm}$ and $\rho_n^c/\rho_n^{ab} \sim 3$ at the onset, the in-plane and out-of-plane penetration lengths, $\lambda_{ab}(T=0) \sim 500 \text{ \AA}$ and $\lambda_c(T=0) \sim 750 \text{ \AA}$, respectively, were determined. Our λ_{ab} is smaller than the reported values [18], but the H -dependence of Z_s is little affected by the absolute value of λ_{ab} . The obtained value of $\lambda_c/\lambda_{ab} \sim 1.5$ is much smaller than the anisotropy of upper critical fields, $H_{c2}^{ab}/H_{c2}^c \simeq 4$ (see the inset of Fig. 2(b)), where H_{c2}^{ab} and H_{c2}^c are the upper critical field in \mathbf{H} parallel to the ab -plane and c -axis, respectively. We note that the small anisotropy of the penetration lengths is consistent with the recent result in Ref. [19].

Figures 2 (a) and (b) show H -dependence of $R_s^{H_\omega \parallel c}$ ($\mathbf{H}_\omega \parallel \mathbf{H} \parallel c$) and $R_s^{H_\omega \parallel ab}$ ($\mathbf{H}_\omega \parallel \mathbf{H} \parallel ab$) measured by Cu-resonator. In both configurations, R_s increase rapidly

with H . In the vortex state, Z_s is determined by vortex dynamics. According to Coffey and Clem, Z_s can be expressed as ,

$$Z_s = i\mu_0\omega\lambda \left[\frac{1 - (i/2)\delta_v^2/\lambda^2}{1 + 2i\lambda^2/\delta_{qp}^2} \right]^{1/2}, \quad (3)$$

where $\delta_v^2 = \delta_f^2(1 - i\omega_p/\omega)^{-1}$, ω_p is the pinning frequency, $\delta_f = \sqrt{2\rho_f/\mu_0\omega}$ is the FFF skin depth, $\delta_{qp} = \sqrt{2\rho_{qp}/\mu_0\omega}$ with the quasi-particle resistivity ρ_{qp} is the normal-fluid skin depth [20]. To estimate the pinning frequency of MgB₂, plots of X_s vs R_s in two configurations are shown in the inset of Fig. 2(a). For comparison, the same data at several ω/ω_p calculated from Eq.(3) are also plotted. The inset of Fig. 2(a) strongly suggests that ω/ω_p is much larger than unity in both configurations, demonstrating that the FFF state is nearly realized in the present frequency range. In the FFF state, two characteristic length scales, namely λ and δ_f , emerge in accordance with microwave penetration. In low fields, λ greatly exceeds δ_f ($\lambda \gg \delta_f$). In this region, R_s and X_s are given by $R_s \simeq \rho_f/\lambda$ and $X_s \simeq \mu_0\omega\lambda$. In high fields where δ_f exceeds λ ($\delta_f \gg \lambda$), the response is similar to the normal state ($R_s \simeq X_s$), except that δ_n is replaced by δ_f . In MgB₂, this cross over occurs at a very low field ($\mu_0 H < 100$ mT) in both configurations. This indicates that the influence of penetration lengths on the vortex dynamics is negligibly small except at very low field regimes.

Having established that the FFF state is realized in the present experiments, FFF resistivities in \mathbf{H} parallel to the c -axis and ab -plane, $\rho_f^{H\parallel c}$ and $\rho_f^{H\parallel ab}$, respectively, are estimated next from Figs.2(a) and (b), assuming $\omega/\omega_p = \infty$. Figure 3 (a) shows $\rho_f^{H\parallel c}$ and $\rho_f^{H\parallel ab}$, normalized by the normal state values as a function of H/H_{c2} at $T=2.3$ K ($T/T_c=0.06$). For comparison, the H -dependence of the FFF resistivity of single gap s -wave superconductor, as given by Eq. (1), and of d -wave Bi:2201, as reported in Ref.[9] are also shown. The field dependence of both $\rho_f^{H\parallel c}$ and $\rho_f^{H\parallel ab}$ are spectacularly different from those of s -wave and d -wave superconductors. Both $\rho_f^{H\parallel c}$ and $\rho_f^{H\parallel ab}$ increase steeply with H at low fields, even steeper than ρ_f in d -wave superconductor. In particular, at $H/H_{c2}^{ab} \simeq 0.1$, $\rho_f^{H\parallel ab}$ of MgB₂ is nearly half of $\rho_f^{H\parallel ab}$ at H_{c2} , indicating a striking enhancement of energy dissipation at very low fields. This unusual FFF state of MgB₂ can be seen more clearly in Fig. 3(b), in which the same data is plotted as a function of $\sqrt{H/H_{c2}}$. A crossover field H_{cr} which separates two distinct flux flow regime with different $\rho_f^{H\parallel ab}$ slope is distinguishable at $\sqrt{H_{cr}/H_{c2}^{ab}} \simeq 0.3$, as indicated by the arrow. On the other hand, such a crossover cannot be easily identified in $\rho_f^{H\parallel c}$.

The appearance of the crossover field can be attributed to the two distinct superconducting gaps. Unusual electronic structure in the vortex state of MgB₂ has been

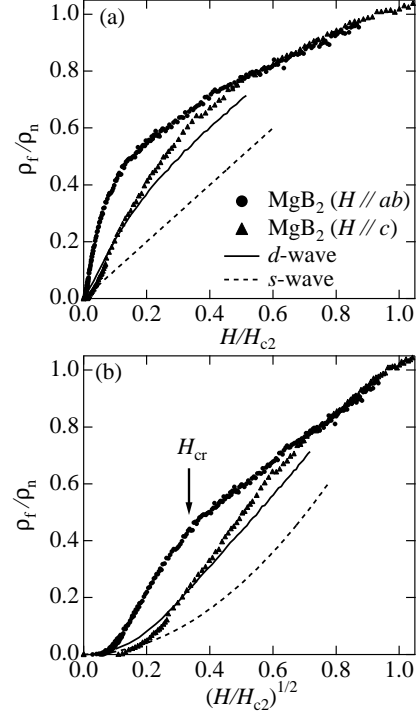


FIG. 3: (a) Flux flow resistivities $\rho_f^{H\parallel c}$ (solid triangles) and $\rho_f^{H\parallel ab}$ (solid circles) at 2.3 K normalized by the normal state values as a function of H normalized by the upper critical fields. The solid line represents the FFF resistivity of conventional s -wave superconductor expressed by Eq. (1). The dashed line represents the FFF resistivity in d -wave superconductor reported in Ref.[9]. (b) The same data plotted as a function of $\sqrt{H/H_{c2}}$.

reported in several experiments. According to STM measurements, the vortex radius is much larger than expected from H_{c2} and superconductivity is strongly suppressed by a low field. Sharp increases in the heat capacity C_e [4] and thermal conductivity κ_e [5] at low fields with initial slopes much larger than in conventional s -wave superconductors also revealed the unusual vortex state of MgB₂. In particular, in $\mathbf{H} \parallel ab$, C_e is nearly half of the normal state value C_e^n at $H/H_{c2}^{ab} \sim 0.1$, followed by a gradual increase up to H_{c2} . Moreover, κ_e in $\mathbf{H} \parallel ab$ becomes nearly H -independent after κ_e reaches nearly half of the normal state value κ_n at $H/H_{c2}^{ab} \sim 0.1$. These strong enhancements of C_e and κ_e at low fields has been attributed to the suppression of the small superconducting gap originating from the three dimensional π -band. Therefore, it is natural to consider that the steep increase and crossover behavior observed in the FFF resistivities could also be attributed to the two superconducting gaps.

In conventional s -wave superconductors, the energy dissipation associated with FFF is caused by the quasi-particles trapped within vortex cores [6, 7]. Since in conventional s -wave superconductors the DOS within cores

is approximately H -independent, FFF resistivity is proportional to the number of vortices as given by Eq.(1). The situation in MgB_2 is very different. Below H_{cr} , quasiparticles are trapped by both small and large gaps. Since the coherence lengths associated with the small gap are much larger than those associated with the large gap, the number of quasiparticles trapped within cores well below H_{cr} is much larger than the number trapped solely by the large gap. This gives rise to strong enhancement of FFF resistivity at low fields. As H approaches H_{cr} , the small gap is strongly suppressed. As a result, the contribution of bound quasiparticles of the π -band essentially becomes negligible above H_{cr} . This gives rise to a gentler increase in FFF resistivity above H_{cr} up to H_{c2} . The kink structure observed at H_{cr} in Fig. 3(b) implies that this crossover occurs in a narrow field range. Similar to the d -wave superconductor described by Eq.(2), $\rho_f^{H\parallel ab}$ below and above H_{cr} exhibit nearly \sqrt{H} dependence. To clarify the origin of this H -dependence, more detailed information on quasiparticle structure and the dissipation mechanism is strongly required.

Recently, the carrier scattering rate in the π -band has been suggested [21, 22] to be much higher than in the σ band. Detailed information about the quasiparticle structure and scattering rate can be extracted when the heat capacity, thermal conductivity and FFF resistivity data are combined. In fact heat capacity is essentially determined by the number of the quasiparticles. On the other hand, thermal conductivity is deter-

mined by delocalized quasiparticles outside vortex cores because localized quasiparticles cannot carry heat. In contrast, energy dissipation in the FFF state is dominated by the quasiparticles localized within cores. We stress that all quantities, heat capacity, thermal conductivity, and FFF resistivity in $H\parallel ab$ follow a striking similar trend; a crossover from low field to high field region occurs at $H_{cr}/H_{c2}^{ab} \simeq 0.1$ and all quantities increase up to nearly half of the normal state values near H_{cr} with $C_e(H_{cr})/C_e(H_{c2}^{ab}) \sim 0.55$, $\kappa(H_{cr})/\kappa(H_{c2}^{ab}) \sim 0.57$, and $\rho_f^c(H_{cr})/\rho_f^c(H_{c2}^{ab}) \sim 0.45$. This implies that *the carrier scattering rate of the σ band is close to that of π the band*. This appears to be inconsistent with the suggestion by Ref.[21, 22]. A more detailed microscopic calculation is needed to evaluate the carrier scattering rate.

In summary, the FFF resistivity in MgB_2 exhibits unusual field dependence, which is markedly different from conventional s -wave superconductors. Two distinct regimes in which the FFF resistivity exhibits different field dependence are observed. These unusual H -dependences indicate that two very differently sized superconducting gaps manifest in energy dissipation associated with the vortex dynamics.

We thank M.B. Gaifullin, N. Hayashi, Y. Kato, T. Kita and E.B. Sonin for valuable discussions. This work was supported by the New Energy and Industrial Technology Development Organization (NEDO) as collaborative research and development of fundamental technologies for superconductivity applications.

-
- [1] J. Nagamatsu, N. Nakagawa, T. Muranaka, Y. Zenitani, and J. Akimitsu, *Nature* **410**, 63 (2001).
 - [2] For the recent review, see P.C. Canfield and G.W. Crabtree, *Physics Today* **56**, 34 (2003).
 - [3] M.R. Eskildsen, M. Kugler, S. Tanaka, J. Jun, S.M. Kazakov, J. Karpinski, and O. Fischer, *Phys. Rev. Lett.* **89**, 187003 (2002).
 - [4] F. Bouquet, R.A. Fisher, N.E. Phillips, D.G. Hinks, and J.D. Jorgensen, *Phys. Rev. Lett.* **87**, 047001 (2001), F. Bouquet, Y. Wang, I. Sheikin, T. Plackowski, and A. Junod, S. Lee, and S. Tajima, *ibid.*, **89**, 257001 (2002).
 - [5] A.V. Sologubenko, J. Jun, S.M. Kazakov, J. Karpinski, and H.R. Ott, *Phys. Rev. B* **66**, 014504 (2002).
 - [6] N.B. Kopnin, *Theory of Nonequilibrium Superconductivity*, (Oxford Science Publishers, Oxford, 2001).
 - [7] M. Eschrig, J.A. Sauls, and D. Rainer, *Phys. Rev. B* **60**, 10447 (1999).
 - [8] S. Kambe, A.D. Huxley, P. Rodiere, and J. Floquet, *Phys. Rev. Lett.* **83**, 1842 (1999).
 - [9] Y. Matsuda, A. Shibata, K. Izawa, H. Ikuta, M. Hasegawa, and Y. Kato, *Phys. Rev. B* **66**, 014527 (2002) and references therein.
 - [10] K. Takaki, A. Koizumi, T. Hanaguri, M. Nohara, H. Takagi, K. Kitazawa, Y. Kato, Y. Tsuchiya, H. Kitano, and A. Maeda, *Phys. Rev. B* **66**, 184511 (2002).
 - [11] K. Izawa, A. Shibata, Y. Matsuda, Y. Kato, H. Takeya, K. Hirata, C.J. van der Beek, and M. Konczykowski, *Phys. Rev. Lett.* **86**, 1327 (2001).
 - [12] Y. Tsuchiya, K. Iwaya, K. Kinoshita, T. Hanaguri, H. Kitano, A. Maeda, K. Shibata, T. Nishizaki, and N. Kobayashi, *Phys. Rev. B* **63**, 184517 (2001).
 - [13] Y. Matsuda, M.B. Gaifullin, K. Kumagai, K. Kadowaki, and T. Mochiku, *Phys. Rev. Lett.* **75**, 4512 (1995).
 - [14] S. Lee, H. Mori, T. Masui, Y. Eltsev, A. Yamamoto and S. Tajima, *J. Phys. Soc. Jpn.* **70**, 2255 (2001).
 - [15] O. Klein, S. Donovan, M. Dressel, and G. Grüner, *Int. J. Infrared and Millimeter Waves* **14**, 2423 (1993).
 - [16] H. Kitano, T. Shibauchi, K. Uchinokura, A. Maeda, H. Asaoka, and H. Takei, *Phys. Rev. B* **51**, 1401 (1995).
 - [17] Yu. Eltsev, K. Nakao, S. Lee, T. Masui, N. Chikumoto, S. Tajima, N. Koshizuka, and M. Murakami, *Phys. Rev. B* **66**, 180504 (2002).
 - [18] A.A. Golubov, A. Brinkman, O.V. Dolgov, J. Kortus, and O. Jepsen, *Phys. Rev. B* **66**, 054524 (2002).
 - [19] R. Cubitt, S. Levett, S.L. Bud'ko, N.E. Anderson, and P.C. Canfield, *Phys. Rev. Lett.* **90**, 157002 (2003).
 - [20] M.W. Coffey and J.R. Clem, *Phys. Rev. Lett.* **67**, 386 (1991).
 - [21] I.I. Mazin, O.K. Andersen, O. Jepsen, O.V. Dolgov, J. Kortus, A.A. Golubov, A.B. Kuz'menko, and D. van der Marel, *Phys. Rev. Lett.* **89**, 107002 (2002).
 - [22] J. W. Quilty, S. Lee, S. Tajima, and A. Yamanaka, *cond-mat/0206506*.